symmetry

MDPI

Article

The Closed-Form Solutions of an SIS Epidemic Reaction–Diffusion Model with Advection in a One-Dimensional Space Domain

Rehana Naz [1] **and Mariano Torrisi** [2,*]

[1] Department of Mathematics and Statistical Sciences, Lahore School of Economics, Lahore 53200, Pakistan; drrehana@lahoreschool.edu.pk
[2] Dipartimento di Matematica e Informatica, Università degli Studi di Catania, Viale Andrea Doria, 6, 95125 Catania, Italy
* Correspondence: torrisi@dmi.unict.it

Abstract: This work investigates a class of susceptible–infected–susceptible (SIS) epidemic model with reaction–diffusion–advection (RDA) by utilizing the Lie group methods. The Lie symmetries are computed for the three widely used incidence functions: standard incidence, mass action incidence, and saturated incidence. The Lie algebra for the SIS-RDA epidemic model is four-dimensional for the standard incidence function, three-dimensional for mass action incidence, and two-dimensional for saturated incidence. The reductions and closed-form solutions for the SIS-RDA epidemic model for the standard incidence infection mechanism are established. The transmission dynamics of an infectious disease utilizing closed-form solutions is presented. To illustrate the paths of susceptible and infected populations, we consider the Cauchy problem. Moreover, a sensitivity analysis is conducted to provide insights into potential policy recommendations for disease control.

Keywords: symmetry methods; susceptible–infected–susceptible; reaction–diffusion–advection; Cauchy problem; standard incidence

check for updates

Citation: Naz, R.; Torrisi, M. The Closed-Form Solutions of an SIS Epidemic Reaction–Diffusion Model with Advection in a One-Dimensional Space Domain. *Symmetry* **2024**, *16*, 948. https://doi.org/10.3390/sym16080948

Academic Editor: Jaume Giné

Received: 4 July 2024
Revised: 21 July 2024
Accepted: 23 July 2024
Published: 24 July 2024

Copyright: © 2024 by the authors. Licensee MDPI, Basel, Switzerland. This article is an open access article distributed under the terms and conditions of the Creative Commons Attribution (CC BY) license (https://creativecommons.org/licenses/by/4.0/).

1. Introduction

A susceptible–infected–susceptible (SIS) compartmental model is governed by a system of 2×2 ordinary differential equations (ODEs). When the spatial movements of both infected and susceptible populations are taken into account, the phenomena are governed by a system of 2×2 reaction–diffusion-type partial differential equations (PDEs). Allen et al. [1], following suggestions from two papers by Fitzgibbon et al. [2,3], introduced an SIS reaction–diffusion model for an epidemic in a continuous spatial habitat. Peng and Liu [4], focused on the global stability of the steady states within an SIS epidemic reaction–diffusion model. Veliov [5] focused on a class of SIS epidemic models in a heterogeneous population. Gudelj et al. [6] investigated how spatial movement and group interactions influence the dynamics of disease spread in social animals using an SIS-type framework for two classes of two social groups.

The biased and/or passive movement behavior can be incorporated into the SIS reaction–diffusion model by adding an advection term. In some realistic environments, populations may exhibit biased or passive movements in certain directions due to external stimuli such as water flow [7], wind [8], and so on. In this framework, several mathematical models have been introduced to understand the effects of migratory movement and spatial heterogeneity on disease transmission. These models are governed by a system of reaction–diffusion–advection (RDA)-type PDEs.

In [9,10], the SIS-RDA epidemic model for the infection mechanism with standard incidence was investigated. Cui et al. [11] analyzed the SIS-RDA model using mass action

and standard rate. Zhang and Cu [12] investigated the SIS-RDA model for the saturated incidence. Ge et al. [13] examined an SIS-RDA epidemic model across different risk domains, providing valuable insights into disease dynamics. Similarly, Rao et al. [14] investigated an SIS epidemic model with a linear external source within a reaction–diffusion–advection framework, contributing to the understanding of disease spread in advective environments. We consider the following class of SIS-RDA system:

$$\begin{cases} S_t = \alpha S_{xx} - \theta S_x - \beta \Phi(S, I) + \gamma I, \\ I_t = \alpha I_{xx} - \theta I_x + \beta \Phi(S, I) - \gamma I, \end{cases} \tag{1}$$

where the infection mechanism $\Phi = \Phi(S, I)$ is given by

$$\Phi(S, I) = \begin{cases} \frac{SI}{S+I}, & \text{standard incidence} \\ SI, & \text{mass action incidence} \\ \frac{SI}{1+mI}, & \text{saturated incidence.} \end{cases}$$

We denote the densities of susceptible and infected populations, with $S(t, x)$ and $I(t, x)$, respectively, at time t and at a location $x \in \mathbf{R}$. The constitutive parameter α denotes the diffusion coefficient for susceptible and infected populations, respectively. θ is the effective speed of the current (sometimes referred to as the advection speed/rate). It should be noted that θ must be non-negative, as x is defined to increase towards the downstream end. β is the infection rate and γ is the recovery/removed rate; both are positive constants.

In the first part of the article, we find the Lie symmetries for the SIS-RDA class represented by (1) for three widely used incidence functions. We apply the symmetry methods to find several reductions and closed-form solutions for SIS-RDA epidemic model (1) for the standard incidence function. It is worth mentioning here that non-linear models governed by a system of PDEs rarely exhibit closed-form solutions. Even if they exist, deriving these solutions is very challenging. Symmetry methods offer a methodological way to get a wide class of exact solutions. The classical books written on symmetry methods are [15–22]. Symmetry methods are effectively employed in several notable works, including [23–27]. Naz et al. [28,29] employed the symmetry methods to establish the closed-form solutions of the diffusive susceptible–infected–recovered (SIR) epidemic model. The book by Cheviakov and Zhao [30] provides a thorough exploration of nonlinear PDEs, delving into their characteristics, computational techniques, and diverse applications within PDE systems. For the computation of Lie symmetries, useful computer packages have been developed [31–33]. In the second part of the article, we solve the Cauchy problem for the SIS-RDA epidemic model for the standard incidence function, detailing the determination of arbitrary constants and the subsequent formulation and analysis of closed-form solutions. We show how the paths of susceptible and infected populations develop over time with parameter values taken from the existing literature. Furthermore, a sensitivity analysis is carried out to provide insights into potential policy recommendations for the control of the disease.

The layout of paper is as follows: the Lie symmetries for the SIS-RDA class represented by class (1) are derived in Section 2. Lie symmetries are established for the standard incidence function, mass action incidence function, and the saturated incidence function. The Lie algebra for the SIS-RDA epidemic model is four-dimensional for the standard incidence function, three-dimensional for mass action incidence, and two-dimensional for saturated incidence. In Section 3, the SIS-RDA epidemic model for the standard incidence function is analyzed in detail. By utilizing the combination of the Lie symmetries, we obtain the reductions and closed-form solutions for the SIS-RDA epidemic model for the standard incidence function. Section 4 is devoted to analyzing the transmission dynamics of an infectious disease by utilizing the derived closed-form solutions. To illustrate the path of susceptible and infected populations, we consider the Cauchy problem. We use graphs to effectively explain the phenomena observed in the model, employing parameter values sourced from the literature. Moreover, we perform a sensitivity analysis in the same

section to provide insights into potential policy recommendations for disease control. The concluding remarks are presented in Section 5.

2. Lie Symmetries for the Class (1)

In this section, we establish the Lie symmetries for the general class of SIS-RDA epidemic model (1) for different infection mechanisms. We consider the three widely used types of incidence functions: standard incidence, mass action incidence, and saturated incidence.

2.1. Symmetry Infinitesimal Operator

A symmetry infinitesimal operator for class (1) has the form

$$X = \tau(t,x,S,I)\partial_t + \xi(t,x,S,I)\partial_t + \eta^1(t,x,S,I)\partial_S + \eta^2(t,x,S,I)\partial_I, \tag{2}$$

where the infinitesimal coordinates ξ^1, ξ^2, η^1, and η^2 are derived from the following invariance conditions:

$$\begin{cases} X^{(2)}(-S_t + \alpha S_{xx} - \theta S_x - \beta\Phi(S,I) + \gamma I)\,|_{(1)} = 0, \\ X^{(2)}(-I_t + \alpha I_{xx} - \theta I_x + \beta\Phi(S,I) - \gamma I)\,|_{(1)} = 0. \end{cases} \tag{3}$$

The operator $X^{(2)}$ is as follows:

$$X^{(2)} = X + \zeta_t^1 \frac{\partial}{\partial_{S_t}} + \zeta_x^1 \frac{\partial}{\partial_{S_x}} + \zeta_{xx}^1 \frac{\partial}{\partial_{S_{xx}}} + \zeta_t^2 \frac{\partial}{\partial_{I_t}} + \zeta_x^2 \frac{\partial}{\partial_{I_x}} + \zeta_{xx}^2 \frac{\partial}{\partial_{I_{xx}}}. \tag{4}$$

As usual, the expressions of the coordinates $\zeta_t^1, \zeta_x^1, \zeta_{xx}^1, \zeta_t^2, \ldots$ are written as (see, e.g., [15–22])

$$\begin{aligned} \zeta_t^1 &= D_t(\eta_1) - S_t D_t(\tau) - S_x D_t(\xi), \\ \zeta_x^1 &= D_x(\eta_1) - S_t D_x(\tau) - S_x D_x(\xi), \\ \zeta_{xx}^1 &= D_x(\zeta_x^1) - S_{xt} D_x(\tau) - S_{xx} D_x(\xi), \\ \zeta_t^2 &= D_t(\eta_2) - I_t D_t(\tau) - I_x D_t(\xi), \\ \zeta_x^2 &= D_x(\eta_2) - I_t D_x(\tau) - I_x D_x(\xi), \\ \zeta_{xx}^2 &= D_x(\zeta_x^2) - I_{xt} D_x(\tau) - I_{xx} D_x(\xi), \end{aligned} \tag{5}$$

where the operators D_x, and D_t are the total derivatives with respect to x and t, respectively.

2.2. Determing System

From (3), after some basic simplifications, we derive the following Lie symmetry determining equations:

$$\begin{aligned} \tau_x = 0, \tau_S = 0, \tau_I = 0, \xi_S = 0, \xi_I = 0, \\ \tau_t - \alpha\tau_{xx} - 2\xi_x + \theta\tau_x = 0, \\ \eta_{SS}^1 = 0, \eta_{II}^1 = 0, \eta_{SI}^1 = 0, \eta_{xI}^1 = 0, \\ \eta_{SS}^2 = 0, \eta_{II}^2 = 0, \eta_{SI}^2 = 0, \eta_{xS}^2 = 0, \\ \xi_t - \theta\xi_x - \alpha\xi_{xx} + 2\alpha\eta_{xI}^2 = 0, \\ \xi_t - \theta\xi_x - \alpha\xi_{xx} + 2\alpha\eta_{xS}^1 = 0, \\ (\beta\Phi - \gamma I)(\eta_S^1 - \eta_I^1 - 2\xi_x) + \gamma\eta^2 - \beta\Phi_S\eta^1 - \beta\Phi_I\eta^2 + \alpha\eta_{xx}^1 - \theta\eta_x^1 - \eta_t^1 = 0, \\ (\beta\Phi - \gamma I)(\eta_S^2 - \eta_I^2 + 2\xi_x) - \gamma\eta^2 + \beta\Phi_S\eta^1 + \beta\Phi_I\eta^2 + \alpha\eta_{xx}^2 - \theta\eta_x^2 - \eta_t^2 = 0. \end{aligned} \tag{6}$$

These equations enable us to determine the form of the infinitesimal components τ, ξ, η^1, and η^2 associated with the different forms of the infection mechanism $\Phi(S,I)$. It is straightforward to find

$$\begin{aligned} \tau = g_1(t),\ \xi = \frac{x}{2}g_1'(t) + g_2(t), \\ \eta^1 = g_3(t)S + g_4(t)I - \frac{S}{4\alpha}\left(\frac{x^2}{2}g_1''(t) - \theta x g_1'(t) + 2x g_2'(t)\right) + G_1(t,x), \\ \eta^2 = g_3(t)I + g_5(t)S - \frac{I}{4\alpha}\left(\frac{x^2}{2}g_1''(t) - \theta x g_1'(t) + 2x g_2'(t)\right) + G_2(t,x), \end{aligned} \tag{7}$$

with constraints

$$\begin{aligned} (\beta\Phi - \gamma I)(\eta_S^1 - \eta_I^1 - 2\xi_x) + \gamma\eta^2 - \beta\Phi_S\eta^1 - \beta\Phi_I\eta^2 + \alpha\eta_{xx}^1 - \theta\eta_x^1 - \eta_t^1 = 0, \\ (\beta\Phi - \gamma I)(\eta_S^2 - \eta_I^2 + 2\xi_x) - \gamma\eta^2 + \beta\Phi_S\eta^1 + \beta\Phi_I\eta^2 + \alpha\eta_{xx}^2 - \theta\eta_x^2 - \eta_t^2 = 0. \end{aligned} \tag{8}$$

It is worth noting that the Lie symmetries for a different incidence coefficient can be derived using Equation (8).

2.3. Lie Symmetries for the Standard Incidence

Consider the standard incidence function

$$\Phi(S,I) = \frac{SI}{S+I}. \tag{9}$$

Using this function in Equation (8), we arrive at the following infinitesimal components:

$$\begin{aligned} \tau = a_1, \xi = a_2 + 2a_3\alpha t, \\ \eta^1 = a_3(t\theta - x)S + a_4 S, \\ \eta^2 = a_3(t\theta - x)I + a_4 I. \end{aligned} \tag{10}$$

The corresponding basis of generators of the four-dimensional Lie algebra for the SIS-RDA system (1) for the standard incidence function are

$$\begin{aligned} X_1 &= \partial_t, \\ X_2 &= \partial_x, \\ X_3 &= 2\alpha t\partial_x + (t\theta - x)S\partial_S + (t\theta - x)I\partial_I, \\ X_4 &= S\partial_S + I\partial_I. \end{aligned} \tag{11}$$

2.4. Lie Symmetries for the Mass Action Incidence

The mass action incidence function is given by

$$\Phi(S,I) = SI. \tag{12}$$

Substituting this function in Equation (8) leads to the following:

$$\begin{aligned} \tau = c_1 + 2c_3\beta t,\ \xi = c_2 + c_3\beta(t\theta + x), \\ \eta^1 = 2c_3(\gamma - \beta S),\ \eta^2 = -2c_3\beta I. \end{aligned} \tag{13}$$

For system (1) with the standard incidence function, the basis of generators of the three-dimensional Lie algebra consists of X_1, X_2, and

$$X_5 = 2\beta t\partial_t + \beta(t\theta + x)\partial_x + 2(\gamma - \beta S)\partial_S - 2\beta I\partial_I. \tag{14}$$

2.5. Lie Symmetries for Saturated Incidence

The saturated incidence function is given by

$$\Phi(S, I) = \frac{SI}{1 + mI}, \tag{15}$$

where $m > 0$ is the saturation coefficient. We solve Equation (8) for saturated incidence (15) and arrive at the two-dimensional Lie algebra for system (1) consisting of X_1 and X_2 only.

3. Reductions and Closed-Form Solutions of the SIS-RDA Epidemic Model for the Standard Incidence Function

In this section, we provide the reductions of the SIS-RDA epidemic model, governed by a system of two second-order nonlinear PDEs, to a system of two nonlinear second-order ODEs by utilizing the most general Lie symmetry operator. We also establish the traveling wave solutions via the linear combination of Lie symmetries X_1 and X_2. Several closed-form solutions are obtained by employing a linear combination of Lie symmetries X_2, X_3, and X_4.

3.1. Reductions of SIS-RDA Epidemic Model to a System of ODEs

The SIS-RDA epidemic model (1) for the standard incidence function takes the following form [9–11]:

$$\begin{cases} S_t = \alpha S_{xx} - \theta S_x - \dfrac{\beta SI}{S + I} + \gamma I, \\ I_t = \alpha I_{xx} - \theta I_x + \dfrac{\beta SI}{S + I} - \gamma I. \end{cases} \tag{16}$$

From the most general symmetry operator

$$X = a_1 X_1 + a_2 X_2 + a_3 X_3 + a_4 X_4 \tag{17}$$

assuming $a_1 \neq 0$, the invariant surface conditions yield the following invariant solutions:

$$\begin{aligned} S(t, x) &= G_1(\chi) e^{\frac{3(\theta a_3 t - 2a_3 x + 2a_4)a_1 t + 4\left(a_3 d_I t + \frac{3}{4} a_2\right) a_3 t^2}{6a_1^2}}, \\ I(t, x) &= G_2(\chi) e^{\frac{3(\theta a_3 t - 2a_3 x + 2a_4)a_1 t + 4\left(a_3 d_I t + \frac{3}{4} a_2\right) a_3 t^2}{6a_1^2}}. \end{aligned} \tag{18}$$

Here, $G_1(\chi)$ and $G_2(\chi)$ are sought as functions of the so called *similarity variable*

$$\chi = \frac{-a_3 d_I t^2 + a_1 x - a_2 t}{a_1},$$

and their forms will be determined by substituting (18) in (16) and solving the following ODE system

$$\begin{cases} -a_1 d_I (G_1 + G_2) G_1'' + (a_1\theta - a_2)(G_1 + G_2) F_1' + (-a_3\chi + a_4) G_1^2 \\ \qquad + (a_1\beta - a_1\gamma - a_3\chi + a_4) G_1 G_2 - a_1\gamma G_2^2 = 0, \\ a_1 d_I (G_1 + G_2) G_2'' - (a_1\theta - a_2)(G_1 + G_2) G_2' + (-a_1\gamma + a_3\chi - a_4) G_2^2 \\ \qquad + (a_1\beta - a_1\gamma + a_3\chi - a_4) G_1 G_2 = 0. \end{cases} \tag{19}$$

In this manner, we map the solution search for (16) onto the solutions of the ODE system (19) described by $G_1(\chi)$ and $G_2(\chi)$.

It is worth noticing that we can obtain several reductions of the SIS-RDA epidemic model (16) by choosing one, two, or three of the constants a_2, a_3, a_4 as zero in the system of reduced second-order ODEs (19). Each specific set of constants a_1, a_2, a_3, a_4 characterizes a combination of Lie symmetries corresponding to a unique reduction. For example, by

choosing $a_2 = 0$ in the system of the reduced second-order ODEs (19), we obtain the reductions via X_1, X_3, and X_4 that are not invariant to the space translations. By adjusting these constants, we expand the scope for reducing the original system, which comprises a system of two second-order PDEs (16) representing the SIS-RDA epidemic model, to a system of two second-order ODEs (19).

3.2. Travelling Waves via X_1 and X_2

The traveling wave-type solutions are invariant with respect to space–time translations admitted by all autonomous equations [34,35]. In our specific case, this translates to the following:

$$S = G_1(\chi), \quad I = G_2(\chi), \quad \chi = x - \frac{a_2}{a_1}t. \tag{20}$$

The following reduced system can be easily obtained in this case by setting $a_3 = a_4 = 0$ in the ODE system (19):

$$\begin{cases} a_1 d_I (G_1 + G_2)G_1'' - (a_1\theta - a_2)(G_1 + G_2)G_1' - (a_1\beta - a_1\gamma)G_1G_2 + a_1\gamma G_2^2 = 0, \\ a_1 d_I (G_1 + G_2)G_2'' - (a_1\theta - a_2)(G_1 + G_2)F_2' + (a_1\beta - a_1\gamma)G_1G_2 - a_1\gamma G_2^2 = 0. \end{cases} \tag{21}$$

Special classes of solutions can be derived from (21) by specifying a_1 and a_2. When $\frac{a_2}{a_1} = \theta$, applying the usual linear combination yields

$$G_1 = G_2 + C_0\chi + C_1 \tag{22}$$

where C_0 and C_1 are arbitrary constants and

$$\begin{aligned} -d_I(2G_2 + C_0\chi + C_1)G_2'' + (\beta - 2\gamma)G_2^2 + (\beta - \gamma)(C_0\chi + C_1)G_2 = 0, \\ d_I(2G_2 + C_0\chi + C_1)G_2'' + (\beta - 2\gamma)G_2^2 + (\beta - \gamma)(C_0\chi + C_1)G_2 = 0. \end{aligned} \tag{23}$$

Equations (22) and (23) provide the final expressions for $G_1(\chi)$ and $G_2(\chi)$ as

$$\begin{aligned} G_1(\chi) &= \frac{\gamma}{2\gamma - \beta}(C_0\chi + C_1), \\ G_2(\chi) &= \frac{\beta - \gamma}{2\gamma - \beta}(C_0\chi + C_1), \end{aligned} \tag{24}$$

provided $\frac{a_2}{a_1} = \theta$ and thus $\chi = x - \theta t$. The final form of traveling wave solutions for the susceptible population $S(t, x)$ and the infected population $I(t, x)$ of the SIS-RDA epidemic model (16) is as follows:

$$\begin{aligned} S(t, x) &= \frac{\gamma}{2\gamma - \beta}\Big(C_0(x - \theta t) + C_1\Big), \\ I(t, x) &= \frac{\beta - \gamma}{2\gamma - \beta}\Big(C_0(x - \theta t) + C_1\Big). \end{aligned} \tag{25}$$

These types of waves are typical of the system as their traveling speed is the same of the advection speed; we could call them advection waves.

3.3. Closed-Form Solutions by Using X_2, X_3, X_4

Now, we derive the closed-form solutions for the SIS-RDA epidemic model (16) by using the linear combination of X_2, X_3, X_4. Here we get the linear combination of X_2, X_3, X_4

by putting $a_1 = 0$ in (17). A similar procedure is carried out as in the previous case to obtain $\chi = t$, and

$$\begin{aligned} S(t,x) &= F_1(t)e^{\frac{x(2a_3\theta t - a_3 x + 2a_4)}{2(2a_3\alpha t + a_2)}}, \\ I(t,x) &= F_2(t)e^{\frac{x(2a_3\theta t - a_3 x + 2a_4)}{2(2a_3\alpha t + a_2)}}, \end{aligned} \tag{26}$$

while the reduced system is as below:

$$\begin{cases} 4\left(a_3\alpha t + \frac{1}{2}a_2\right)^2 F_1' + \Big[t\alpha(\theta^2 t + 2\alpha)a_3^2 + a_2a_3(\theta^2 t + \alpha) \\ +a_2a_4\theta - a_4^2\alpha\Big]\frac{F_1^2}{F_1+F_2} - 4\Big[\left(\gamma\alpha t - \beta\alpha t - \frac{1}{2}\alpha - \frac{1}{4}\theta^2 t\right)\alpha t a_3^2 + \\ \left(-\frac{1}{4}\theta^2 t - \frac{1}{4}\alpha + \gamma t\alpha - \beta t\alpha\right)a_2a_3 + \frac{1}{4}a_4^2\alpha + \frac{1}{4}a_2(-\beta a_2 + \gamma a_2 - a_4\theta)\Big]\frac{F_1F_2}{F_1+F_2} \\ -4\gamma\left(a_3\alpha t + \frac{1}{2}a_2\right)^2\frac{F_2^2}{F_1+F_2} = 0, \\ \\ (2a_3\alpha t + a_2)^2 F_2' + \Big[\left(4t\gamma\alpha + 2\alpha + \theta^2 t\right)\alpha t a_3^2 - a_4^2\alpha + \\ \left(4t\gamma\alpha + \theta^2 t + \alpha\right)a_2a_3 + a_2(a_2\gamma + a_4\theta)\Big]\frac{F_2^2}{F_1+F_2} \\ +\Big[\left(\theta^2 t + 2\alpha + 4\gamma t\alpha - 4\beta t\alpha\right)\alpha t a_3^2 + \left(\alpha + 4\gamma\alpha t - 4\beta\alpha t + \theta^2 t\right)a_2a_3 \\ -a_4^2\alpha + a_2(\gamma a_2 - \beta a_2 + a_4\theta)\Big]\frac{F_1F_2}{F_1+F_2} = 0. \end{cases} \tag{27}$$

3.3.1. Closed-Form Solution for $a_3 \neq 0$

The general solution of Equation (27) for $a_3 \neq 0$ where a_2 and a_4 can be zero or non-zero is

$$\begin{aligned} F_1(t) &= \frac{\left(e^{-(\beta-\gamma)t}C_1\beta - C_2\gamma\right)e^{-\frac{2a_3\alpha\theta^2 t(2a_3\alpha t + a_2) + (a_2\theta - 2a_4\alpha)^2}{8\alpha^2 a_3(2a_3\alpha t + a_2)}}}{\sqrt{2a_3\alpha t + a_2}\left(e^{-(\beta-\gamma)t}C_1 - C_2\right)C_2}, \\ F_2(t) &= \frac{(\gamma-\beta)e^{-\frac{2a_3\alpha\theta^2 t(2a_3\alpha t + a_2) + (a_2\theta - 2a_4\alpha)^2}{8\alpha^2 a_3(2a_3\alpha t + a_2)}}}{\sqrt{2a_3\alpha t + a_2}\left(e^{-(\beta-\gamma)t}C_1 - C_2\right)}. \end{aligned} \tag{28}$$

Substituting $F_1(t)$ and $F_2(t)$ from (28) into (26), we obtain the final expressions for the closed-form solutions for the susceptible population $S(t,x)$ and the infected population $I(t,x)$ of the SIS-RDA epidemic model (16) as follows:

$$\begin{aligned} S(t,x) &= \frac{\left(e^{-(\beta-\gamma)t}C_1\beta - C_2\gamma\right)e^{-\frac{4(\theta t - x)^2 a_3^2\alpha^2 - 8xa_3a_4\alpha^2 + 2a_2a_3\theta^2\alpha t + (a_2\theta - 2a_4\alpha)^2}{8\alpha^2 a_3(2a_3\alpha t + a_2)}}}{\sqrt{2a_3\alpha t + a_2}C_2\left(e^{-(\beta-\gamma)t}C_1 - C_2\right)}, \\ I(t,x) &= \frac{(\gamma-\beta)e^{-\frac{4(\theta t - x)^2 a_3^2\alpha^2 - 8xa_3a_4\alpha^2 + 2a_2a_3\theta^2\alpha t + (a_2\theta - 2a_4\alpha)^2}{8\alpha^2 a_3(2a_3\alpha t + a_2)}}}{\sqrt{2a_3\alpha t + a_2}\left(e^{-(\beta-\gamma)t}C_1 - C_2\right)}. \end{aligned} \tag{29}$$

It is worth emphasizing that the closed-form solution of the diffusive SIS epidemic reaction–diffusion model (16), presented in Equation (29), provides the benchmark for deriving closed-form solutions using different combinations of Lie symmetries X_2, X_3, and X_4. More precisely, it corresponds to the closed-form solution achieved using the Lie symmetry X_3 when both a_2 and a_4 are set to zero. Furthermore, the closed-form solution (29) yields the solution which corresponds to the closed-form solution obtained through the combination of the Lie symmetries X_2 and X_3 when a_4 is set to zero. Similarly, the closed-form solution

involving the combination of Lie symmetries X_3 and X_4 can be deduced by setting a_2 to zero.

3.3.2. Closed-Form Solution for $a_3 = 0, a_2 \neq 0$

Equation (26) for the $a_3 = 0, a_2 \neq 0$ case simplifies to

$$\begin{aligned} S(t,x) &= F_1(t)e^{\frac{a_4}{a_2}x}, \\ I(t,x) &= F_2(t)e^{\frac{a_4}{a_2}x}, \end{aligned} \tag{30}$$

and the general solution of the system of ODEs (27) is

$$\begin{aligned} F_1(t) &= \frac{e^{-\frac{a_4(a_2\theta - a_4\alpha)t}{a_2^2}}\left(e^{-(\beta-\gamma)t}C_1\beta - C_2\gamma\right)}{C_2(e^{-(\beta-\gamma)t}C_1 - C_2)}, \\ F_2(t) &= \frac{e^{-\frac{a_4(a_2\theta - a_4\alpha)t}{a_2^2}}(\gamma-\beta)}{e^{-(\beta-\gamma)t}C_1 - C_2}, \end{aligned} \tag{31}$$

where a_4 can be zero or non-zero.

The substitution of $F_1(t)$ and $F_2(t)$ from Equation (31) into Equation (30) yields the closed-form solutions for the susceptible population $S(t,x)$ and the infected population $I(t,x)$ of the SIS-RDA epidemic model (16) as follows:

$$\begin{aligned} S(t,x) &= \frac{e^{\frac{a_2a_4(x-\theta t)+a_4^2\alpha t}{a_2^2}}\left(e^{-(\beta-\gamma)t}C_1\beta - C_2\gamma\right)}{C_2(e^{-(\beta-\gamma)t}C_1 - C_2)}, \\ I(t,x) &= \frac{e^{\frac{a_2a_4(x-\theta t)+a_4^2\alpha t}{a_2^2}}(\gamma-\beta)}{e^{-(\beta-\gamma)t}C_1 - C_2}. \end{aligned} \tag{32}$$

It is worth emphasizing that the closed-form solution of the SIS-RDA epidemic model (16), presented in Equation (32), provides a solution via X_2 when we set constant $a_4 = 0$.

This completes the search for all closed-form solutions of the SIS-RDA epidemic model (16) via different combinations of Lie symmetries.

4. The Transmission Dynamics of an Infectious Disease Utilizing the Closed-Form Solutions

In this section, we find the closed-form solution for the SIS-RDA epidemic model satisfying Cauchy's problem. Next, we explore the derived closed-form solution that satisfies Cauchy's problem for a real-world scenario to analyze the transmission dynamics of an infectious disease. The closed-form solution is visually illustrated using parameter values from the literature. Sensitivity analysis is performed to examine the effect of changes in the diffusion coefficient and advection rate.

4.1. A Cauchy Problem

A Cauchy problem for system (16) in the domain $D \equiv [0,+\infty) \times [0,+\infty)$ is characterized as follows: The initial conditions are assumed to be

$$\begin{cases} S(0,x) = S_0\Omega(x), \\ I(0,x) = I_0\Omega(x), \\ \qquad x \in [0,+\infty) \end{cases} \tag{33}$$

where the scaling constants I_0 and S_0 represent the initial densities (at $t = 0$) of susceptible and infected populations and $\Omega(x)$ describes the initial distributions of susceptible and

infected populations across the spatial domain. Applying the initial conditions (33) to the group-invariant solution (30) yields

$$F_1(0) = S_0,\ F_2(0) = I_0, \tag{34}$$

and the following expression for the initial distributions of susceptible and infected populations $\Omega(x)$ across the domain:

$$\Omega(x) = e^{-\lambda x}, \lambda > 0. \tag{35}$$

It is straightforward to determine that we must choose $a_4 = -\lambda$ and $a_2 = 1$, which means the linear combination of symmetries $X_2 - \lambda X_4$ is used to construct this solution. Applying the initial conditions of (34) to the general solution for $F_1(t)$ and $F_2(t)$ provided in (31), we have

$$\begin{aligned} \frac{\beta C_1 - \gamma C_2}{C_2(C_1 - C_2)} &= S_0, \\ \frac{\gamma - \beta}{C_2(C_1 - C_2)} &= I_0, \end{aligned} \tag{36}$$

which yields

$$\begin{aligned} C_1 &= \frac{(\gamma - \beta)S_0 + \gamma I_0}{(S_0 + I_0)I_0}, \\ C_2 &= \frac{\beta}{S_0 + I_0}. \end{aligned} \tag{37}$$

Substituting the value of constants C_1 and C_2 from Equation (37) into $F_1(t)$ and $F_2(t)$ provided in (31), we have

$$\begin{aligned} F_1(t) &= \frac{(S_0 + I_0)\Big(((\gamma - \beta)S_0 + \gamma I_0)e^{-(\beta-\gamma)t} - \gamma I_0\Big)e^{\lambda(\theta+\lambda\alpha)t}}{\Big((\gamma - \beta)S_0 + \gamma I_0\Big)e^{-(\beta-\gamma)t} - \beta I_0}, \\ F_2(t) &= \frac{(\gamma - \beta)(S_0 + I_0)I_0 e^{\lambda(\theta+\lambda\alpha)t}}{\Big((\gamma - \beta)S_0 + \gamma I_0\Big)e^{-(\beta-\gamma)t} - \beta I_0}. \end{aligned} \tag{38}$$

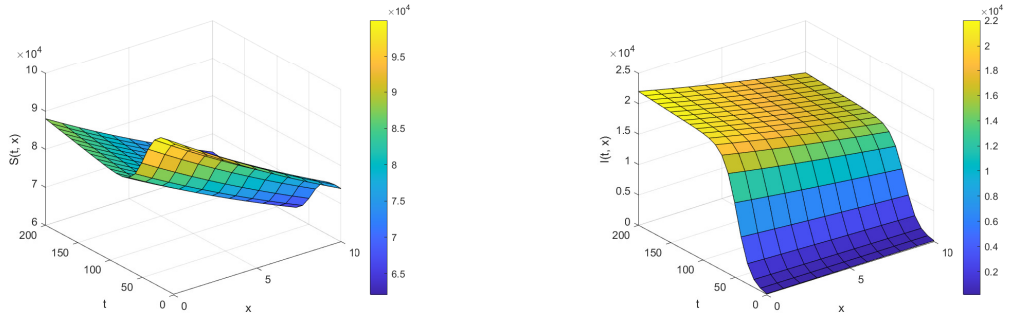
Substituting the values of $F_1(t)$ and $F_2(t)$ from (38) into (30), the final form of the group-invariant solution for $S(t, x)$ and $I(t, x)$ satisfying the Cauchy problem (33) is

$$\begin{aligned} S(t,x) &= \frac{(S_0 + I_0)\Big(((\gamma - \beta)S_0 + \gamma I_0)e^{-(\beta-\gamma)t} - \gamma I_0\Big)e^{\lambda(\theta+\lambda\alpha)t-\lambda x}}{\Big((\gamma - \beta)S_0 + \gamma I_0\Big)e^{-(\beta-\gamma)t} - \beta I_0}, \\ I(t,x) &= \frac{(\gamma - \beta)(S_0 + I_0)I_0 e^{\lambda(\theta+\lambda\alpha)t-\lambda x}}{\Big((\gamma - \beta)S_0 + \gamma I_0\Big)e^{-(\beta-\gamma)t} - \beta I_0}. \end{aligned} \tag{39}$$

4.2. Visualization of Closed-Form Solutions

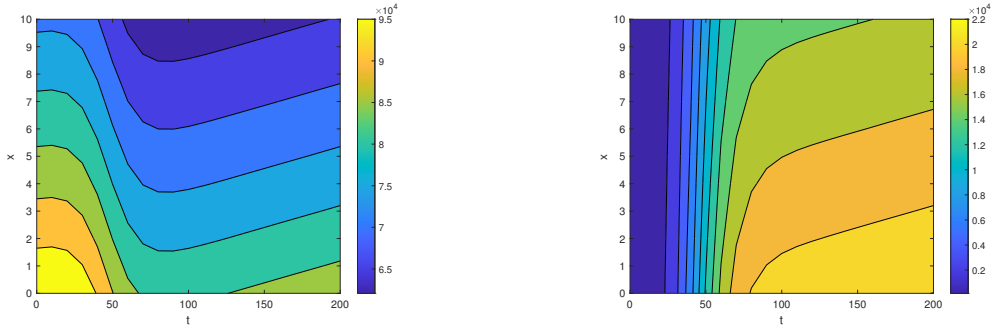
Next, we examine the closed-form solutions for the densities of a susceptible population S and infected population I as given in Equation (39). Specific parameter values sourced from the existing epidemiology literature (see, e.g., [28,29] and the references therein) are utilized. The selected benchmark values of parameter values are $S_0 = 10^5 - 200$, $I_0 = 200$, $\lambda = 0.03$, $\alpha = 0.2$, $\beta = 0.5$, $\gamma = 0.4$, and $\theta = 0.01$. We consider the spatial range $0 \leq x \leq 10$ and the time interval $0 \leq t \leq 200$ to visualize the closed-form solutions (39) graphically. Benchmark values play a vital role in numerical simulations for performing a sensitivity analysis for the epidemic models. All other parameters are set at the benchmark

level while one or more parameters are changed to analyze their impact on the suspected and infected populations. It is important to mention here that the closed-form solution (39) can be rigorously tested across different parameter settings, not limited to those included here. The surface plots of the densities of the susceptible population $S(t,x)$ and infected population $I(t,x)$ are provided in Figure 1. The contour maps of the densities of susceptible and infected populations are provided in Figure 2. Figures 3 and 4 present 2D plots showing susceptible and infected populations for the fixed values of $x = 0, 6, 8, 10$.



(**a**) (**b**)

Figure 1. The density plot for (**a**) $S(t,x)$ and (**b**) $I(t,x)$ for $S_0 = 10^5 - 200$, $I_0 = 200$, $\lambda = 0.03$, $\alpha = 0.2$, $\beta = 0.5$, $\gamma = 0.4$, and $\theta = 0.01$ over the time intervals $0 \leq t \leq 200$ and $0 \leq x \leq 10$.



(**a**) (**b**)

Figure 2. The contour map for (**a**) $S(t,x)$ and (**b**) $I(t,x)$ for $S_0 = 10^5 - 200$, $I_0 = 200$, $\lambda = 0.03$, $\alpha = 0.2$, $\beta = 0.5$, $\gamma = 0.4$, and $\theta = 0.01$ over the time intervals $0 \leq t \leq 200$ and $0 \leq x \leq 10$.

First, we analyze the behavior of the susceptible population $S(t,x)$ from Figures 1a, 2a, and 3. At the disease source, located at $x = 0$, the susceptible population initially decreases before showing an upward trend after a certain period, indicating a long-term increase. This same pattern is observed at other locations such as $x = 6, 8, 10$. The number of susceptible individuals is highest at $x = 0$ and decreases as we move away from the disease source. Specifically, the graphs show the highest susceptibility at $x = 0$ and the lowest at $x = 10$.

Our analysis now shifts to the density of the infected population $I(t,x)$ highlighted in Figures 1b, 2b, and 4. At the disease source located at $x = 0$, the number of infected individuals initially increases before taking a sudden turn after a certain period, continuing to increase steadily thereafter. A similar pattern is observed at other locations such as $x = 6, 8, 10$. The highest number of infected individuals is observed at $x = 0$, and the count decreases as we move away from the disease source. Specifically, the graphs show the highest number of infections at $x = 0$ and the lowest at location $x = 10$.

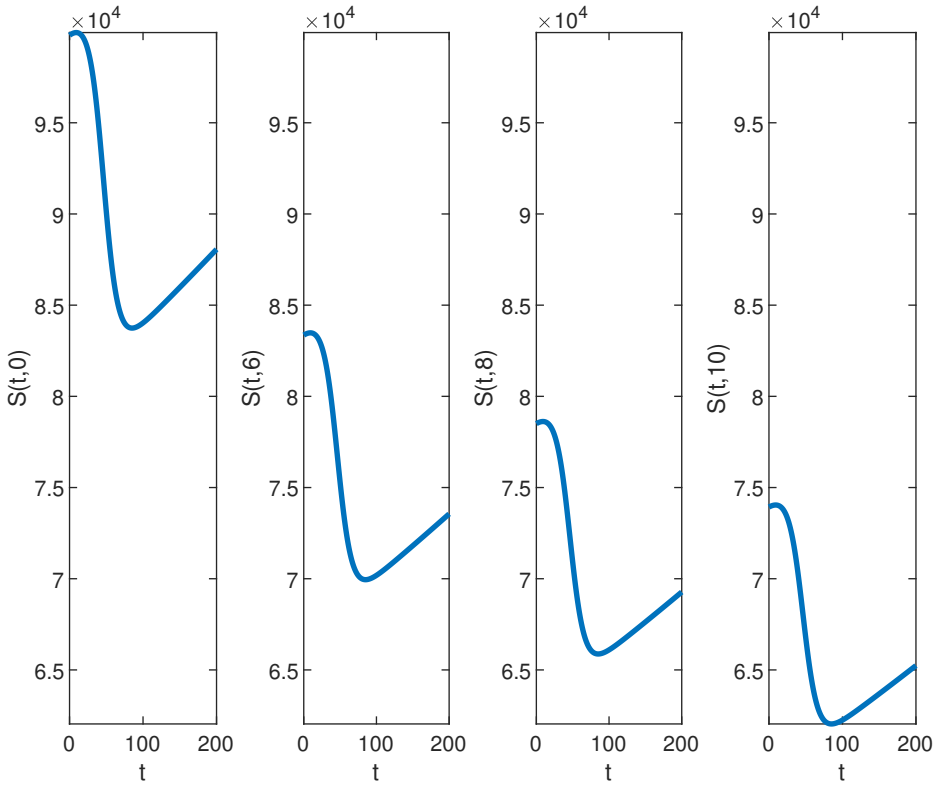


Figure 3. The graph of $S(t, \bar{x})$ for $S_0 = 10^5 - 200$, $I_0 = 200$, $\lambda = 0.03$, $\alpha = 0.2$, $\beta = 0.5$, $\gamma = 0.4$, and $\theta = 0.01$ over the time interval $0 \leq t \leq 200$ and for fixed values of $x = 0, 6, 8, 10$.

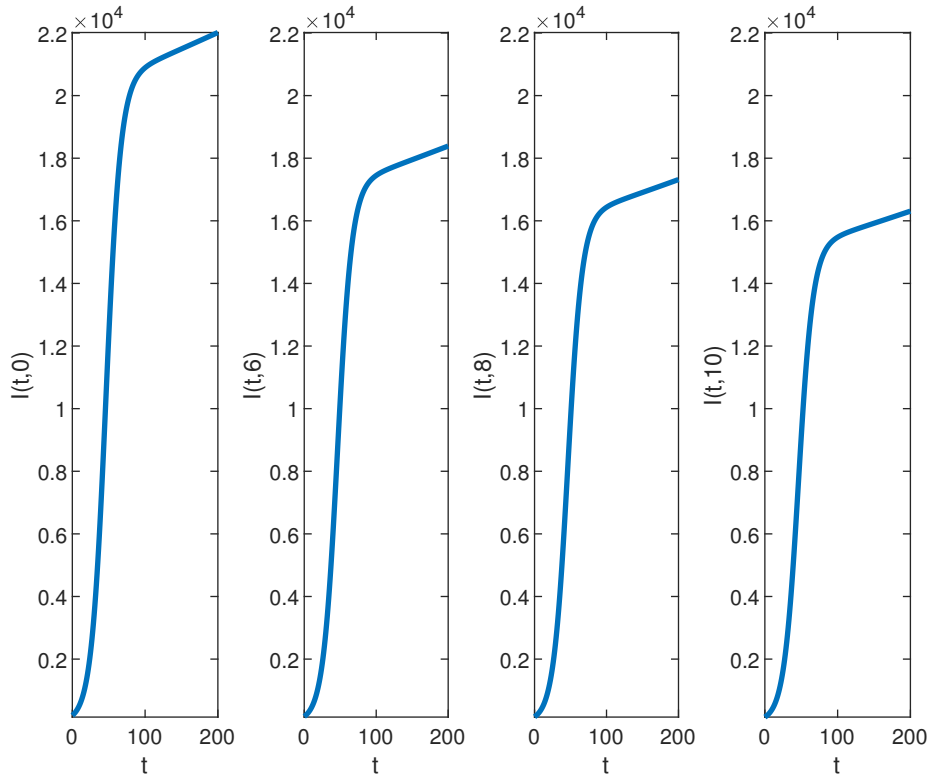
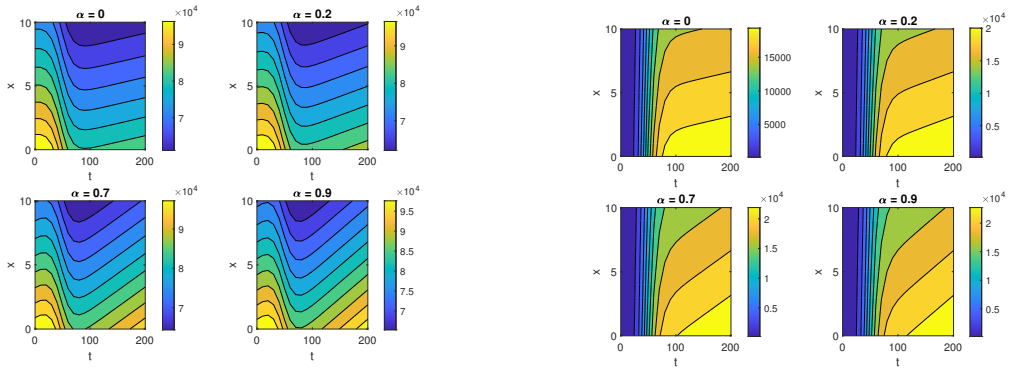


Figure 4. The graph of $I(t, \bar{x})$ for $S_0 = 10^5 - 200$, $I_0 = 200$, $\lambda = 0.03$, $\alpha = 0.2$, $\beta = 0.5$, $\gamma = 0.4$, and $\theta = 0.01$ over the time interval $0 \leq t \leq 200$ and fixed values of $x = 0, 6, 8, 10$.

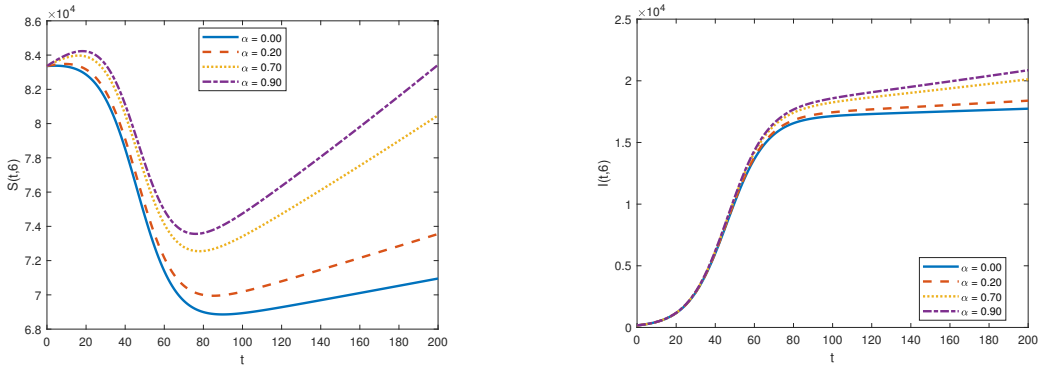
4.3. Effect of Varying the Diffusion Coefficient on Susceptible and Infected Populations

Figures 5 and 6 illustrate the impact of varying the diffusion coefficient, denoted as α, on both susceptible and infected populations. The increase in the diffusion coefficient leads to a higher influx of individuals into the susceptible compartment, reflecting an increased movement of people into the location from external sources. Shifting our focus to the infected compartment, it is evident that the infected population also rises with the increase in the diffusion coefficient. This makes sense, as the movement of infected individuals contributes to the transmission of the infection to previously healthy individuals.



(**a**) $S(t,x)$ (**b**) $I(t,x)$

Figure 5. The contour maps for (**a**) $S(t,x)$ and (**b**) $I(t,x)$ for different diffusion coefficients α.



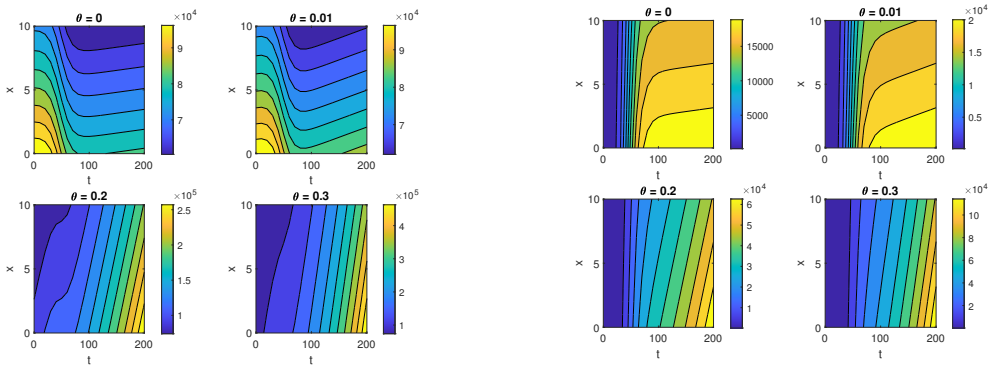
(**a**) (**b**)

Figure 6. The graph of (**a**) $S(t,6)$ and (**b**) $I(t,6)$ for different diffusion coefficients α.

4.4. Effect of Varying the Advection Rate on Susceptible and Infected Populations

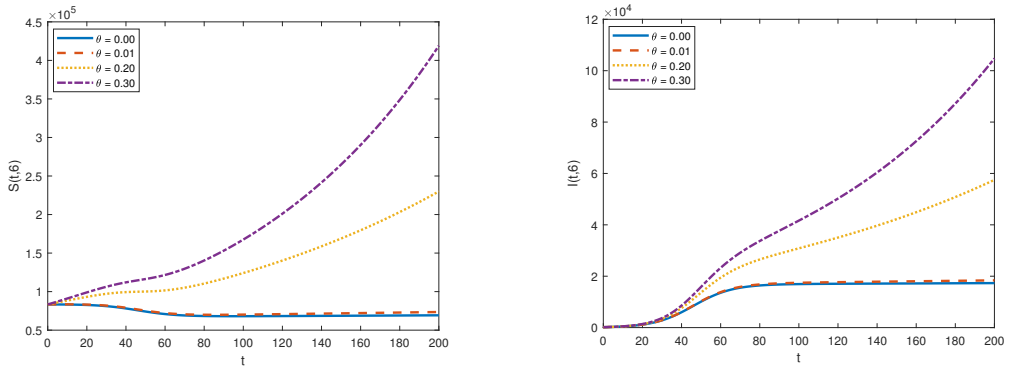
Figures 7 and 8 illustrate the impact of varying the advection rate, denoted as θ, on both susceptible and infected populations. For smaller values of the advection rate, such as $\theta = 0$ and $\theta = 0.01$, the susceptible population initially decreases and then stabilizes. Shifting our focus to the infected compartment, for these same smaller advection rates, the infected population initially increases and then stabilizes. This pattern is logical as individuals leave the susceptible compartment and enter the infected compartment. Over time, due to better disease management and precautionary measures, both the susceptible and infected populations stabilize.

Shifting our focus to the higher values of the advection rate, both the susceptible and infected populations increase. This significant rise in the advection rate results in a greater influx of individuals into the susceptible compartment, reflecting the heightened movement of people into the location from external sources. It is clear that the infected population also rises with the increase in the advection rate. This is expected, as the movement of infected individuals facilitates the transmission of the infection to previously healthy individuals.



(**a**) $S(t,x)$ (**b**) $I(t,x)$

Figure 7. The contour maps for (**a**) $S(t,x)$ and (**b**) $I(t,x)$ for a different advection velocity θ.



(**a**) (**b**)

Figure 8. The graph of (**a**) $S(t,6)$ and (**b**) $I(t,6)$ for a different advection velocity θ.

5. Conclusions

This work explored a class of SIS epidemic model with reaction–diffusion–advection by utilizing the Lie group methods. Lie symmetries were established for three widely utilized incidence functions: standard, mass action, and saturated. The SIS-RDA model exhibited a four-dimensional Lie algebra with the standard incidence function, a three-dimensional Lie algebra with mass action incidence, and a two-dimensional Lie algebra with saturated incidence.

The investigation of the SIS-RDA epidemic model for the standard incidence infection mechanism was extended. We explored several reductions and closed-form solutions by employing linear combinations of Lie symmetries. The transmission dynamics of an infectious disease utilizing closed-form solutions were presented. The solution to the Cauchy problem provided insights into the trajectories of susceptible and infected populations. We showed how the paths of susceptible and infected populations develop over time with parameter values sourced from the existing literature. Furthermore, a sensitivity analysis was conducted to provide insights into potential policy recommendations for the control of the disease.

It is worth mentioning here that we have tested the closed-form solution for a set of parameter values taken from the literature. Parameter values from the data of any specific country can be employed to analyze the derived closed-form solution and understand the transmission dynamics of the infectious disease.

Author Contributions: Conceptualization, R.N. and M.T.; Methodology, R.N. and M.T.; Software, R.N. and M.T.; Formal analysis, R.N. and M.T.; Investigation, R.N. and M.T.; Resources, R.N. and M.T.; Writing—original draft, R.N. and M.T.; Writing—review and editing, R.N. and M.T.; Visualization, R.N. and M.T. All authors have read and agreed to the published version of the manuscript.

Funding: This research received no external funding.

Data Availability Statement: Data is contained within the article.

Acknowledgments: M.T. performed this paper in the framework of G.N.F.M. of INdAM.

Conflicts of Interest: The author declares no conflicts of interest.

References

1. Allen, L.J.S.; Bolker, B.M.; Lou, Y.; Nevai, A.L. Asymptotic profiles of the steady states for an SIS epidemic reaction-diffusion model. *Discret. Contin. Dyn. Syst.* **2008**, *21*, 1–20. [CrossRef]
2. Fitzgibbon, W.E.; Langlais, M.; Morgan, J.J. A mathematical model of the spread of feline leukemia virus (FeLV) through a highly heterogeneous spatial domain. *SIAM J. Math. Anal.* **2001**, *33*, 570–588. [CrossRef]
3. Fitzgibbon, W.E.; Langlais, M.; Morgan, J.J. A reaction-diffusion system modeling direct and indirect transmission of diseases. *Discrete Contin. Dyn. Syst. Ser. B* **2004**, *4*, 893–910. [CrossRef]
4. Peng, R.; Liu, S. Global stability of the steady states of an SIS epidemic reaction-diffusion model. *Nonlinear Anal. Theory Methods Appl.* **2009**, *71*, 239–247. [CrossRef]
5. Veliov, V.M. On the effect of population heterogeneity on dynamics of epidemic diseases. *J. Math. Biol.* **2005**, *51*, 123–143. [CrossRef]
6. Gudelj, I.; White, K.A.J.; Britton, N.F. The effects of spatial movement and group interactions on disease dynamics of social animals. *Bull. Math. Biol.* **2004**, *66*, 91–108. [CrossRef] [PubMed]
7. Lutscher, F.; Lewis, M.A.; McCauley, E. Effects of heterogeneity on spread and persistence in rivers. *Bull. Math. Biol.* **2006**, *68*, 2129–2160. [CrossRef]
8. Desai, M.M.; Nelson, D.R. A quasispecies on a moving oasis. *Theor. Popul. Biol.* **2005**, *67*, 33–45. [CrossRef]
9. Cui, R.; Lou, Y. A spatial SIS model in advective heterogeneous environments. *J. Differ. Equ.* **2016**, *261*, 3305–3343. [CrossRef]
10. Jiang, D.; Wang, Z.C.; Zhang, L. A reaction-diffusion-advection SIS epidemic model in a spatially-temporally heterogeneous environment. *Discret. Contin. Dyn. Syst. Ser. B* **2018**, *23*, 4557–4578. [CrossRef]
11. Cui, R.; Li, H.; Peng, R.; Zhou, M. Concentration behavior of endemic equilibrium for a reaction-diffusion-advection SIS epidemic model with mass action infection mechanism. *Calc. Var. Partial. Differ. Equ.* **2021**, *60*, 184. [CrossRef]
12. Zhang, J.; Cui, R. Asymptotic behavior of an SIS model with saturation and spontaneous infection mechanism. *Z. Angew. Math. Phys.* **2020**, *71*, 1–21. [CrossRef]
13. Ge, J.; Kim, K.I.; Lin, Z.; Zhu, H. A SIS-advection model in a low-risk and high-risk domain. *J. Differ. Equ.* **2015**, *259*, 5486–5509. [CrossRef]
14. Rao, X.; Zhang, G.; Wang, X. A reaction-diffusion-advection SIS epidemic model with linear external source and open advective environments. *Discret. Contin. Dyn. Syst. Ser. B* **2022**, *27*, 6655–6677. [CrossRef]
15. Bluman, G.W.; Cole, J.D. *Similarity Methods for Differential Equations*; Springer: New York, NY, USA, 1974.
16. Ovsiannikov, L.V. *Group Analysis of Differential Equations*; Academic Press: New York, NY, USA, 1982.
17. Ibragimov, N.H. *Transformation Groups Applied to Mathematical Physics*; Reidel: Dordrecht, The Netherlands, 1985.
18. Olver, P.J. *Applications of Lie Groups to Differential Equations*; Springer: New York, NY, USA, 1986.
19. Bluman, G.W.; Kumei, S. *Symmetries and Differential Equations*; Springer: Berlin, Germany, 1989.
20. Ibragimov, N.H. *CRC Handbook of Lie Group Analysis of Differential Equations*; CRC Press: Boca Raton, FL, USA, 1996.
21. Cantwell, B.J. *Introduction to Symmetry Analysis*; Cambridge University Press: Cambridge, UK, 2002.
22. Ibragimov, N.H. *A Practical Course in Differential Equations and Mathematical Modelling*; World Scientific Publishing Co Pvt Ltd.: Singapore, 2009.
23. Senthilvelan, M.; Torrisi, M. Potential symmetries and new solutions of a simplified model for reacting mixtures. *J. Phys. A Math. Gen.* **2000**, *33*, 405. [CrossRef]
24. Torrisi, M.; Tracinà, R. An application of equivalence transformations to reaction diffusion equations. *Symmetry* **2015**, *7*, 1929–1944. [CrossRef]
25. Wang, G. A new (3 + 1)-dimensional Schrödinger equation: Derivation, soliton solutions and conservation laws. *Nonlinear Dyn.* **2021**, *104*, 1595–1602. [CrossRef]
26. Cherniha, R.M.; Davydovych, V.V. A reaction-diffusion system with cross-diffusion: Lie symmetry, exact solutions and their applications in the pandemic modelling. *Eur. J. Appl. Math.* **2022**, *33*, 785–802. [CrossRef]
27. Freire, I.L.; Da Silva, P.L.; Torrisi, M. Lie and Noether symmetries for a class of fourth-order Emden-Fowler equations. *J. Phys. A Math. Theor.* **2013**, *46*, 245206. [CrossRef]
28. Naz, R.; Johnpillai, A.; Mahomed, F.M.; Omame, A. Closed-form solutions for a reaction-diffusion SIR model with different diffusion coefficients. *Discret. Contin. Dyn. Syst. Ser. S* **2024**. . [CrossRef]
29. Naz, R.; Johnpillai, A.; Mahomed, F.M. The exact solutions of a diffusive SIR model via symmetry groups. *J. Math.* **2024**, *2024*, 4598831. [CrossRef]
30. Cheviakov, A.F.; Zhao, P. *Analytical Properties of Nonlinear Partial Differential Equations: With Applications to Shallow Water Models*; Springer Nature: Berlin/Heidelberg, Germany, 2024; Volume 10.

31. Hereman, W. Symbolic software for Lie symmetry analysis. In *CRC Handbook of Lie Group Analysis of Differential*; CRC: Boca Raton, FL, USA, 1996; Volume 3, pp. 367–413.
32. Hereman, W. Review of symbolic software for Lie symmetry analysis. *Math. Comput. Model.* **1997**, *25*, 115–132. [CrossRef]
33. Cheviakov, A.F. GeM software package for computation of symmetries and conservation laws of differential equations. *Comput. Phys. Commun.* **2007**, *176*, 48–61. [CrossRef]
34. Takahashi, L.T.; Maidana, N.A.; Ferreira, W.C.; Pulino, P.; Yang, H.M. Mathematical models for the Aedes aegypti dispersal dynamics: Travelling waves by wing and wind. *Bull. Math. Biol.* **2005**, *67*, 509–528. [CrossRef]
35. Bacani, F.; Dimas, S.; Freire, I.L.; Maidana, N.A.; Torrisi, M. Mathematical modelling for the transmission of dengue: Symmetry and travelling wave analysis. *Nonlinear Anal. Real World Appl.* **2018**, *41*, 269–287. [CrossRef]

Disclaimer/Publisher's Note: The statements, opinions and data contained in all publications are solely those of the individual author(s) and contributor(s) and not of MDPI and/or the editor(s). MDPI and/or the editor(s) disclaim responsibility for any injury to people or property resulting from any ideas, methods, instructions or products referred to in the content.